Electronic Supplementary Material (ESI) for Nanoscale.
This journal is © The Royal Society of Chemistry 2017

Engineering exchange bias and the bias temperature in single phase $Bi_9Fe_5Ti_3O_{27}$ through modulating the spin glassy state

Guopeng Wang[1], He Yang[1], Jianlin Wang[3,4], Shujie Sun[1], Zhengping Fu[2,1,3], Xiaofang Zhai[2,3], Ranran Peng[1,2,3,4], Randy J. Knize,[5] Yalin Lu[2,1,3,4*,5]*

[1]CAS Key Laboratory of Materials for Energy Conversion, Department of Materials Science and Engineering, University of Science and Technology of China, Hefei 230026, P. R. China

[2] Hefei National Laboratory for Physical Sciences at Microscale, University of Science and Technology of China, Hefei 230026, P. R. China

[3] Synergetic Innovation Center of Quantum Information & Quantum Physics, University of Science and Technology of China, Hefei, Anhui 230026, China

[4] National Synchrotron Radiation Laboratory, University of Science and Technology of China, Hefei 230026, P. R. China

[5] Laser Optics Research Center, US Air Force Academy, Colorado 80840, USA

Supplementary Results

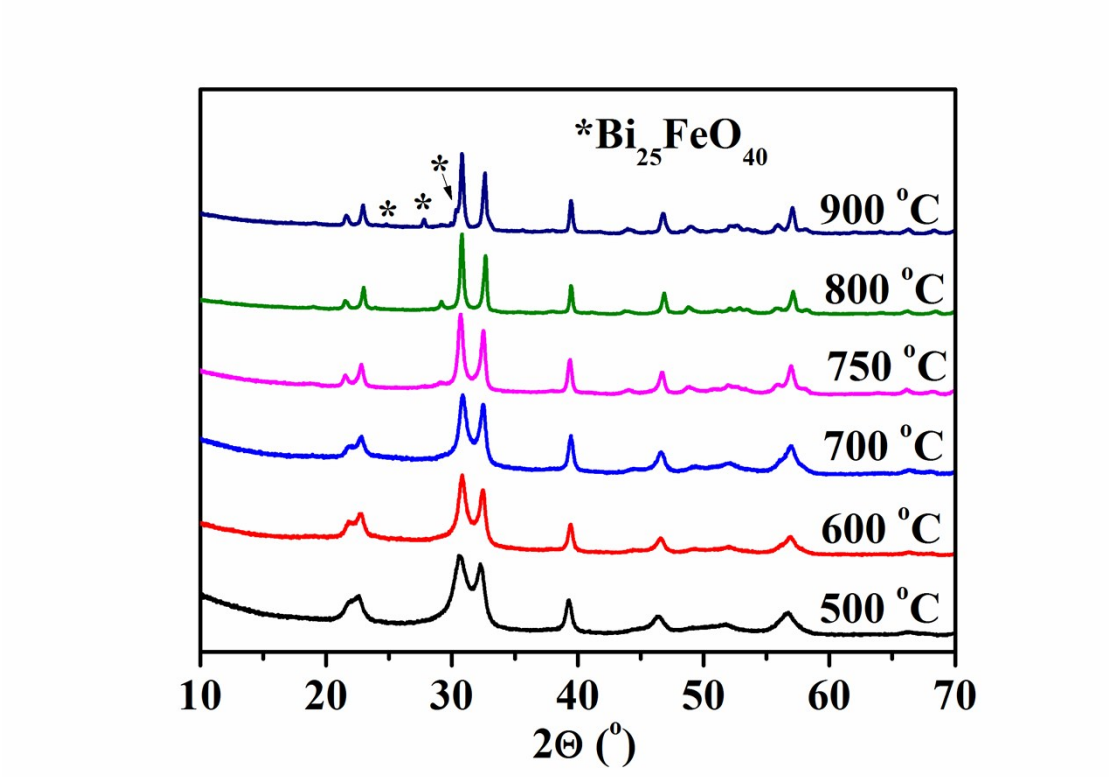

Fig. S1 XRD patterns of BFT samples.

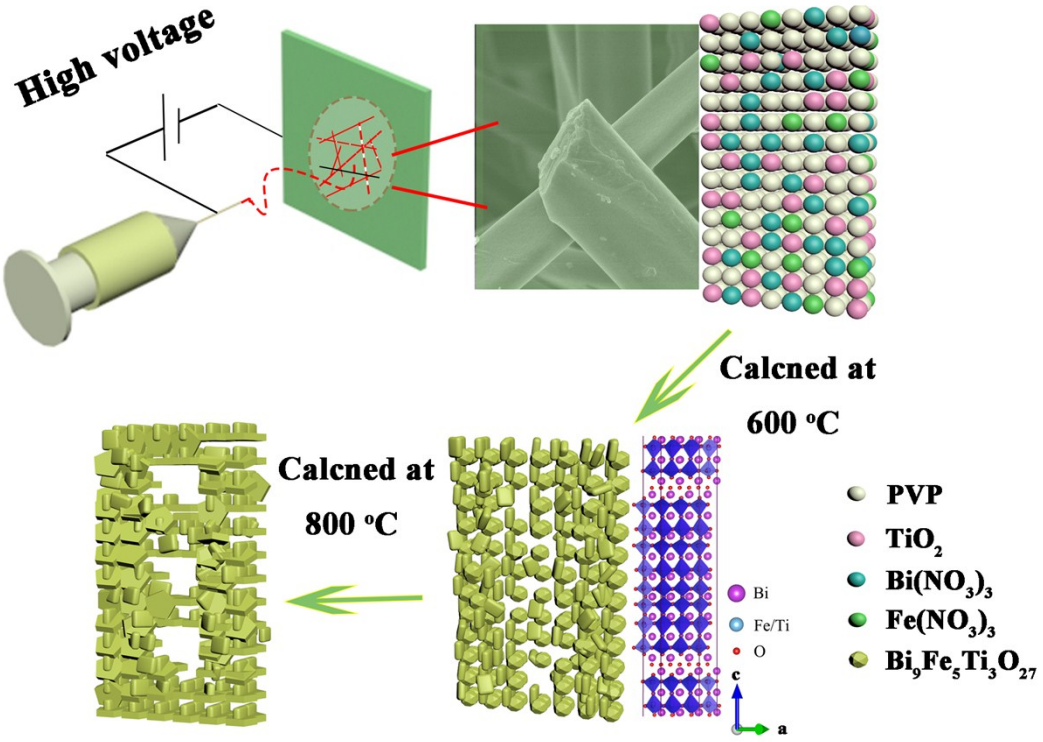

Fig. S2 Schematic illustration for the formation process of BFT nanofibers.

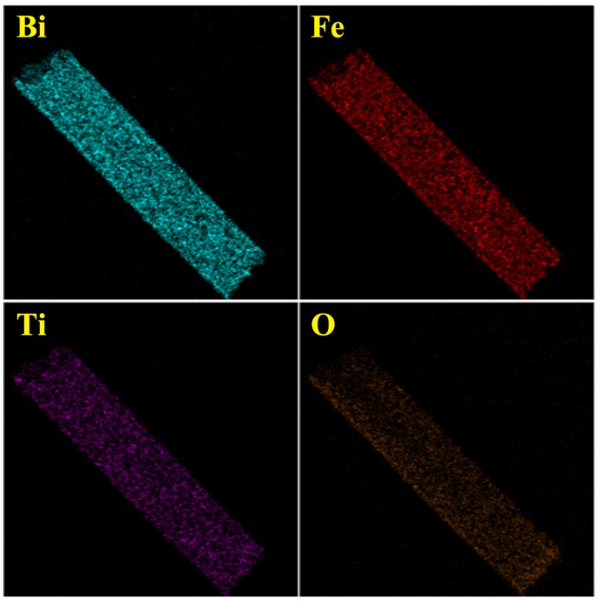

Fig. S3 EDS mappings of an individual BFT-600 nanobelt. Elements of Bi, Fe, Ti and O are evenly distributed throughout the single nanobelt.

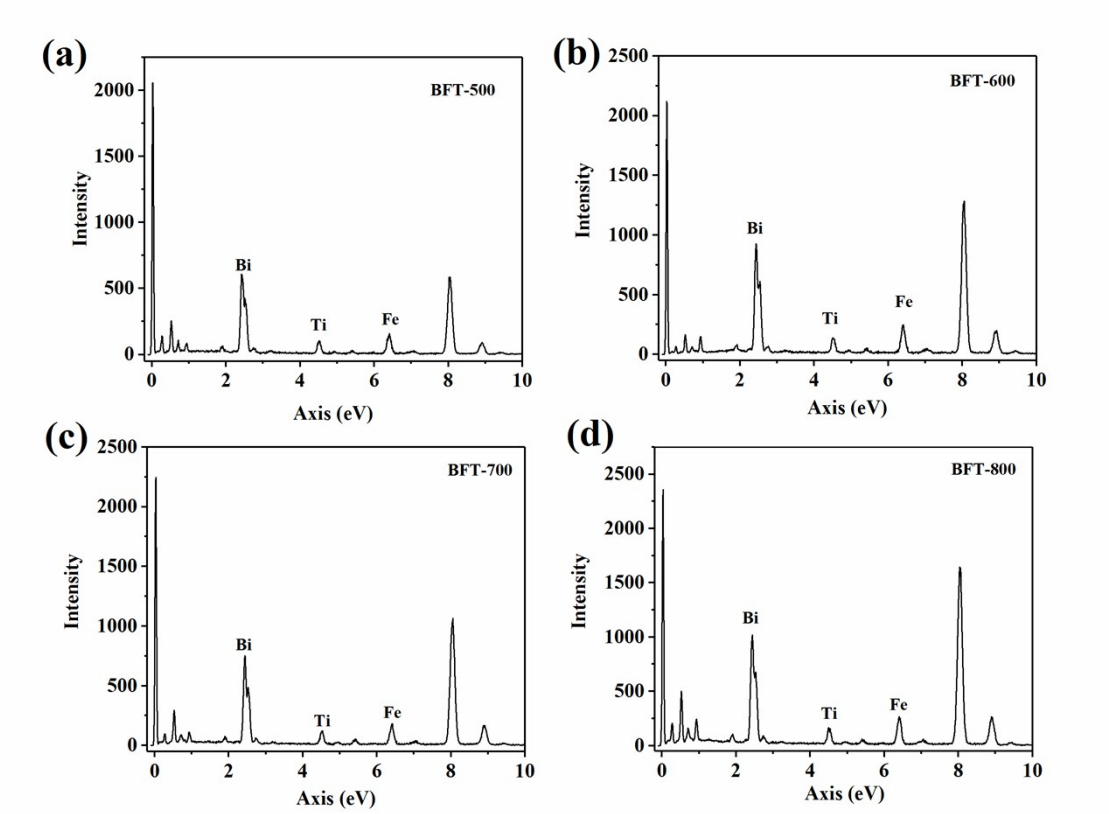

Fig. S4 EDS images of BFT-x samples.

Elements of Bi, Fe and Ti can be detected in four samples, and the relative mole ratio of metal elements in each sample are listed in Table S1.

Table S1 Relative mole ratios of Bi and Fe to Ti (with Ti mole ratio fixed as 3) in BFT-x samples.

Samples	Bi	Fe
BFT-500	9.75	4.71
BFT-600	9.79	4.57
BFT-700	9.72	4.53
BFt-800	9.89	4.64

As shown in table S1, four samples possess similar elements mole ratio which implies that the mole ratio of metal elements in BFT-x samples should not account for the

difference in their magnetic behavior.

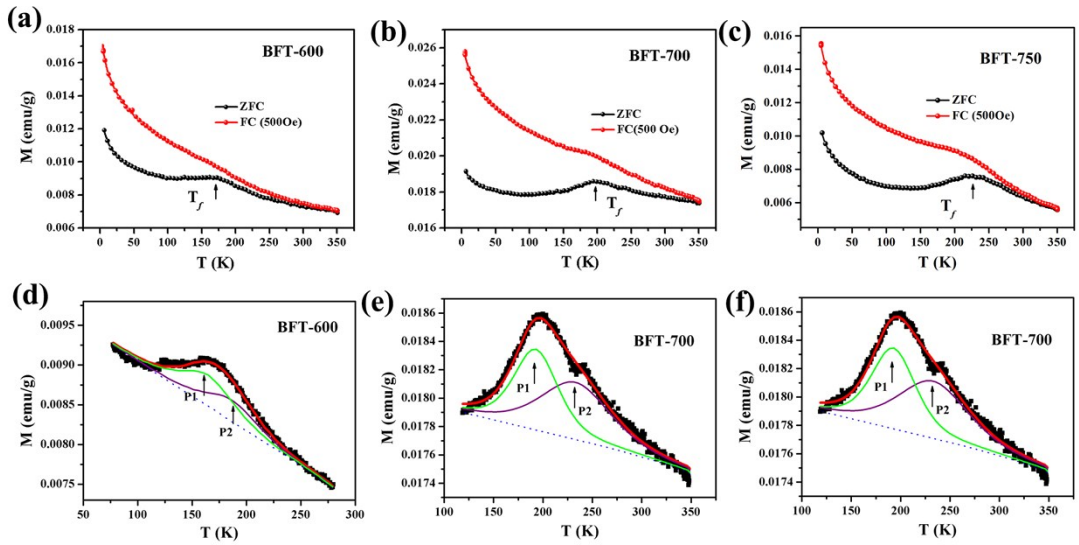

Fig. S5 Temperature dependences of the ZFC and FC curves (a) BFT-600, (b) BFT-700 and (c) BFT-750. (d-f) The fit curves of spin glass peak of ZFC plots (d) BFT-600, (e) BFT-700 and (f) BFT-750.

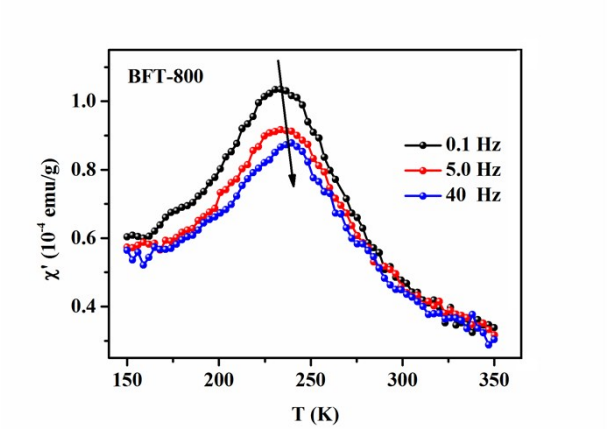

Fig. S6 The temperature dependences of the real part χ' of AC susceptibility for BFT-800 at different frequencies without a dc field.

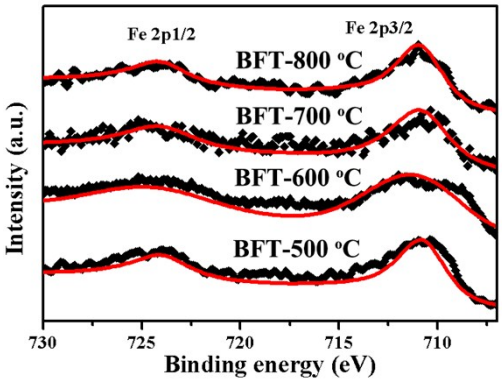

Fig. S7 Typical XPS spectra of Fe 2p core levels for BFT-500, BFT-600, BFT-700 and BFT-800 samples. From the results which can be observed that only two peaks locating at 724.01 and 710.76 eV are observed, which are very close to the binding energy of Fe 2p1/2 (724.00 eV) and Fe 2p3/2 (711.00 eV) in Fe_2O_3.[S1]

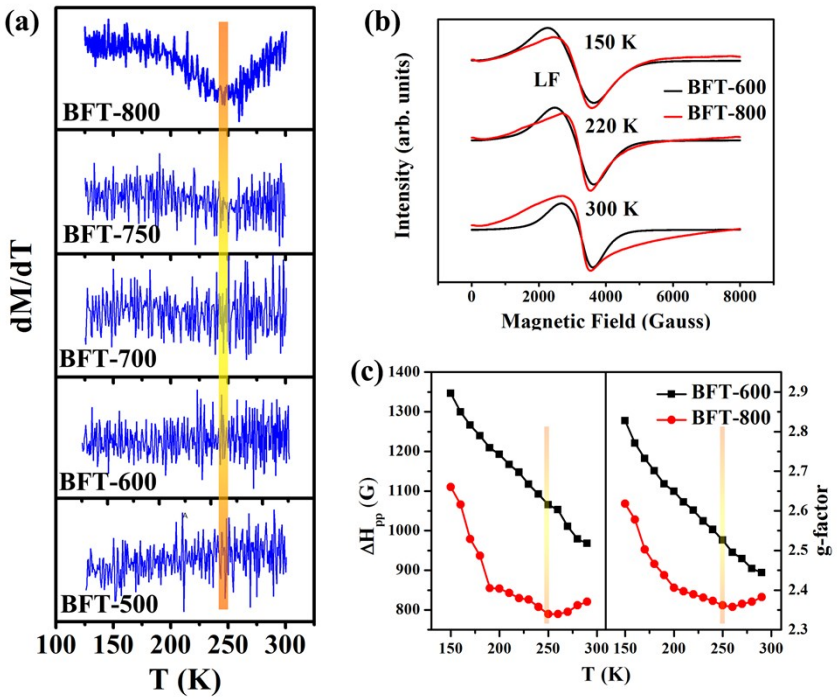

Fig. S8 (a) The plots of dM/dT vs. T based on the data of M_{FC} of all the BFT samples. (b) EPR measurements of BFT-600 and BFT-800 samples at various temperatures. (c) Temperature dependence of peak-to-peak linewidth $\triangle H_{pp}$ and LF associates with the g-factor of BFT-600 and BFT-800 samples.

Fig. S6b† shows the EPR spectrum of BFT-600 and BFT-800 samples measured from 150 to 290 K. Two resonances segments, i.e., low field (LF) and high field (HF) resonance shoulders, can be observed in the EPR resonance. We can see that calcination temperature has an remarkable effects over the EPR spectrum, of which both the linewidth ($\triangle H_{pp}$), closely related to the spin-spin relaxation time and the spin-phonon relaxation time, and LF associates with the g-factor for the BFT-800 are smaller than that of BFT-600 in the whole measured temperature range, as shown in Fig. S6c.† For BFT-600, the linewidth increase almost linearly with the depressed temperatures, while for BFT-800 sample, the linewidth reduces first with decreasing temperature and then increases, with a minimum value achieved at a temperature around 250 K, which is very close to the AFM transition temperature acquired from dM/dT curve. Here, the broadening of peak below 250 K may be associated with a critical "slowing down" of the spin fluctuations in ferromagnets when AFM transition temperature is approached from above,[S1] while that above 250K, increase of $\triangle H_{pp}$ may come from the improved interaction of spin-lattice at enhanced temperatures. From the g-factor results, we also can see anomaly in BFT-800 sample at about 250 K while for BFT-600 is not, and the g-factor for the BFT-800 is smaller than that of BFT-600 in almost temperature range maybe caused by the decreased magnetization. Both the EPR spectrum and the dM/dT curves indicate that BFT-800 has different spinning state along with different temperature independence with BFT-600, highly suggesting that with the reduce of particle size, the uncompensated spins increases and thus weakens the AFM interaction leading to the faded AFM transition.

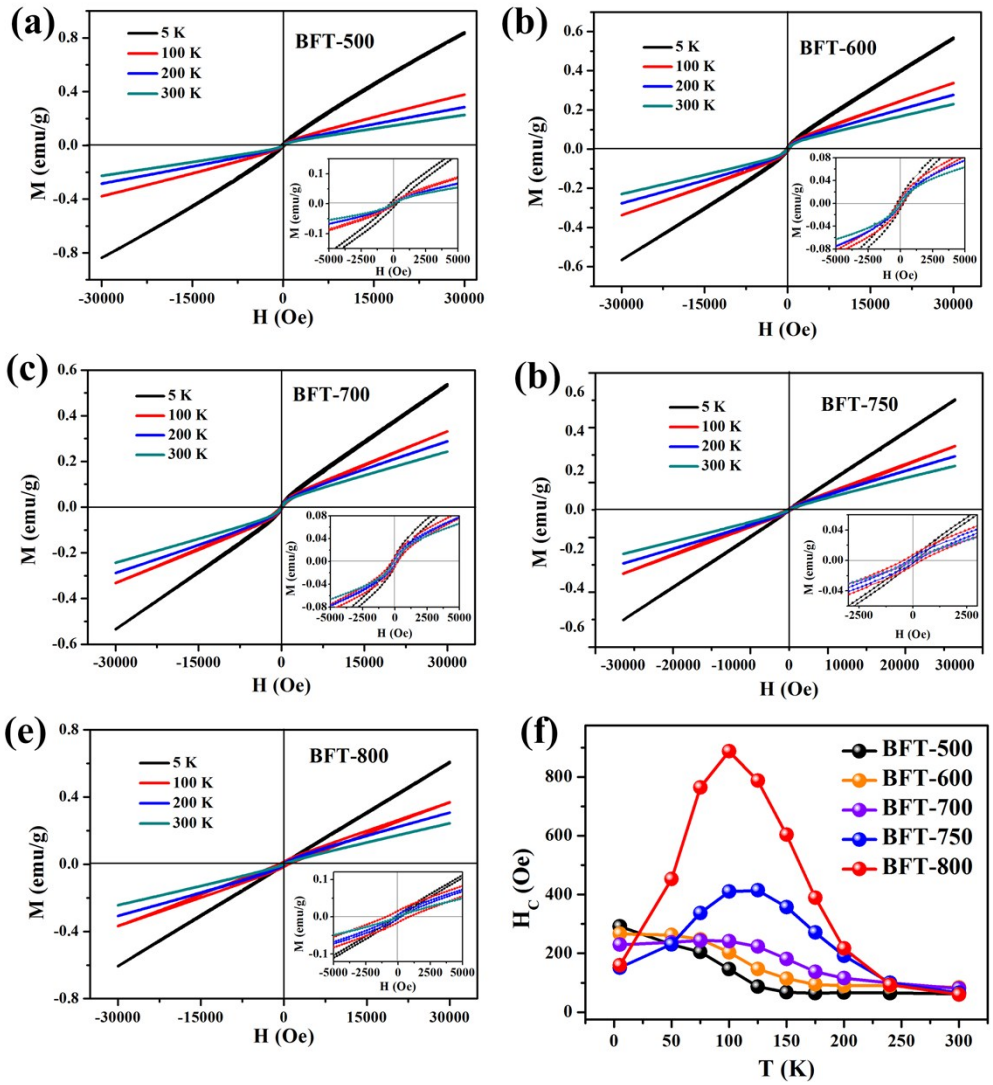

Fig. S9 The M-H curves of (a) BFT-500, (b) BFT-600, (c) BFT-700, (d) BFT-750 and (e) BFT-800 measured at different temperatures ranging from 5 K to 300 K. (d) Temperature dependence of H_C for all the BFT samples.

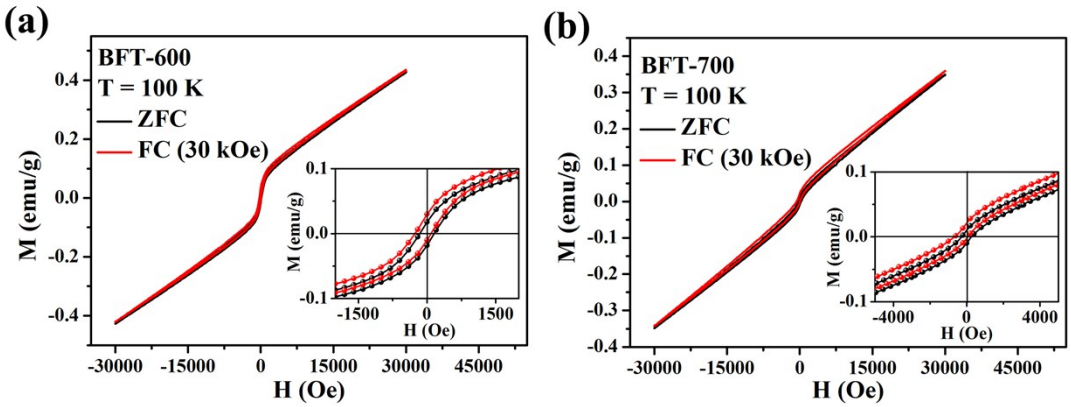

Fig. S10 Typical M-H curves of, BFT-600 (a) and BFT-700 (b) sample measured at 100 K when cooling in ZFC and FC (30 kOe) modes.

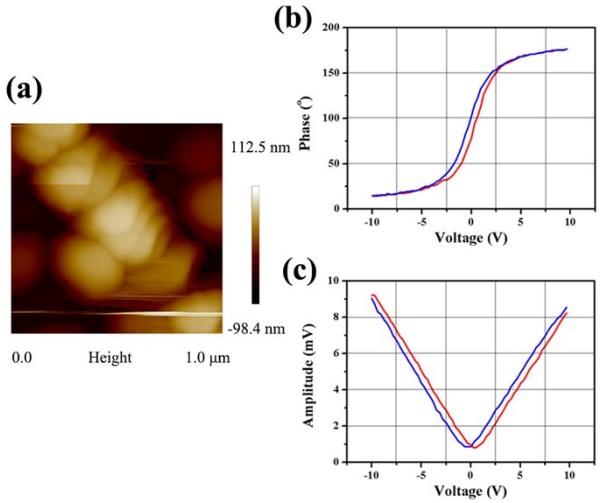

Fig. S11 Piezoresponse force microscopy (PFM) of BFT-700 sample (a) PFM topography image, (b) phase and (c) amplitude local response under DC bias.

Reference

(S1) X. Y. Cheng, X. X. Wang, H. S. Yang, K. Q. Ruan and X. G. Li, *J. Mater. Chem C*., 2015, **3**, 4482-4501.

(S2) A. Shengelaya, G. M. Zhao, H. Keller, K. A. Müller, *Phys. Rev. Lett.*, 1996, **77**, 5296-5299.